JOURNAL OF THERMOPHYSICS AND HEAT TRANSFER
Vol. 11, No. 3, July–September 1997

Correlation Transfer: Index of Refraction and Anisotropy Effects

N. M. Reguigui*
Centre National des Sciences et Technologies Nucléaires, Cedex 1080, Tunis, Tunisia
and
F. Dorri-Nowkoorani,† U. Nobbmann,‡ B. J. Ackerson,§ and R. L. Dougherty¶
Oklahoma State University, Stillwater, Oklahoma 74078

The derivation of a correlation transfer equation is outlined. This correlation transfer equation comes from multiple-scattering theory for the electric field fluctuations of light propagating through suspensions of diffusing particles. The correlation equation is very similar to the radiative intensity equation. Thus, radiative solution techniques are applied to obtain results for isotropic and anisotropic one-dimensional media. For anisotropic scattering, a forward-scattering approximation is used along with the preaveraging method for handling the single-scattering correlation function. Transmitted and backscattered results are presented. Theoretical results are also presented for detection in directions other than direct backscattering or direct transmission, and results are presented for the effect of refractive index. These predictions are compared with another published theory and with experimental data for an expanded 514.5-nm laser beam scattering from suspensions of 0.107-, 0.304-, and 0.497-μm diameter polystyrene latex spheres. For intermediate optical thicknesses, preaveraging theory yields good agreement with the experimental data presented if the effects of refractive index are included in the theory. For small optical thickness, polarization effects are important and need to be included in the future to yield acceptably accurate predictions.

Nomenclature

a_t = total cross section, m^2
D_0 = Stokes–Einstein diffusion constant of spherical particles in a medium, $k_BT/(3\pi\eta d)$, m^2/s
d = diameter of particles diffusing by Brownian motion through a medium, m
$d\Omega$ = differential solid angle around the direction $\hat{\Omega}$
$E(\boldsymbol{r}_a, t)$ = scalar electric field at the location $\boldsymbol{r}_a$ and time t, N/C
f = fraction of forward scattering, Eq. (20)
f = field scattering amplitude, Eq. (4)
G^m = multiple-scattering field correlation function
G_i^m = multiple-scattering field correlation function at the inner boundary of a medium
g^1 = single-scattering field correlation function
I = specific coherent intensity of radiation, $W\ m^{-2}\ Sr^{-1}\ Hz^{-1}$
i = $\sqrt{-1}$
K = medium's effective wave number, m^{-1}
$\boldsymbol{K}$ = medium's effective wave vector ($|\boldsymbol{K}| = K$), Eq. (5), m^{-1}
k = free medium's wave number, m^{-1}
$\boldsymbol{k}$ = free medium's wave vector ($|\boldsymbol{k}| = k = 2\pi n/\lambda$), m^{-1}
k_B = Boltzmann constant, $J\ K^{-1}$
L_0 = nominal optical thickness of medium, $\sigma_t \underline{z}_0$
N = number of particles in the scattering volume
n = ratio of refractive index inside medium to index outside medium
P = phase function for single scattering
$\boldsymbol{q}$ = wave vector, Fourier transform variable
R = Fresnel's reflection coefficient
$\boldsymbol{r}$ = $(\boldsymbol{r}_a + \boldsymbol{r}_b)/2$, m
$\boldsymbol{r}_a, \boldsymbol{r}_b$ = position vectors (or observation points) in space between particles, m
$\boldsymbol{r}_d$ = $(\boldsymbol{r}_a - \boldsymbol{r}_b)$, m
$\boldsymbol{r}_s$ = $(\boldsymbol{r}_{s'} + \boldsymbol{r}_{s''})/2$, m
$\boldsymbol{r}_{s'}, \boldsymbol{r}_{s''}$ = position vectors for a moving particle at two different times ($t_{s'}$ and $t_{s''}$), m
$\boldsymbol{r}_{sd}$ = $(\boldsymbol{r}_{s'} - \boldsymbol{r}_{s''})$, m
$\boldsymbol{r}_0$ = position vector on the boundary of medium under consideration, m
s = parameter used in Fresnel's equation
T = temperature of the medium, K
t = time, s
U = total intensity, $W\ m^{-1}\ Hz^{-1}$
V = function defined in Eq. (3)
w = probability function
z = optical coordinate
z_0 = maximum optical coordinate, i.e., true optical thickness, $\sigma_t \underline{z}_0(1 - f)(1 + 2\pi/\tau_0)$
$\underline{z}$ = physical coordinate, m
$\underline{z}_0$ = maximum physical coordinate, m
$\Gamma(\boldsymbol{r}, \boldsymbol{r}_d, t)$ = mutual coherence function, $\langle E(\boldsymbol{r}_a, t_a)E^*(\boldsymbol{r}_b, t_b)\rangle$, N^2/C^2
$\Gamma(\boldsymbol{r}, \boldsymbol{q}, \tau)$ = spectral density in q space, Eq. (8), $N^2\ m^3/C^2$
δ = Dirac delta
η = viscosity of medium, Pa s
Θ = scattering angle
θ = polar angle, measured to the inward normal to the medium boundary
λ = wavelength, m

Presented as Paper 93-0141 at the AIAA 31st Aerospace Sciences Meeting, Reno, NV, Jan. 11–14, 1993; received Sept. 20, 1996; revision received Jan. 31, 1997; accepted for publication Feb. 1, 1997.

*Assistant d'Enseignement Supérieur, Département des Sciences et Technologie Nucléaires, BP 204.
†Research Associate in Physics.
‡Research Assistant in Physics.
§Regents Professor of Physics.
¶Professor of Mechanical and Aerospace Engineering. Associate Fellow AIAA.

$\boldsymbol{\mu}$ = cosine of the polar angle
$\boldsymbol{\rho}(\boldsymbol{r})$ = number density, number of scatterers per unit volume at $\boldsymbol{r}$, m^{-3}
σ_a = absorption coefficient, m^{-1}
σ_s = scattering coefficient, m^{-1}
σ_t = extinction coefficient, $\sigma_a + \sigma_s$, m^{-1}
τ = correlation delay time, s
τ_0 = characteristic time, $1/D_0K_r^2$, s
$\boldsymbol{\phi}_i(\boldsymbol{r}_a)$ = unscattered incident wave at $\boldsymbol{r}_a$, N/C
$\hat{\boldsymbol{\Omega}}$ = unit vector in the scattered direction
$\hat{\boldsymbol{\Omega}}'$ = unit vector in the incident direction, or in the direction of propagation
ω = single-scattering albedo, σ_s/σ_t
ω_e = effective delay time-dependent albedo
$*$ = complex conjugate
$\langle\ \rangle$ = ensemble average
$\hat{}$ = unit vector
$\tilde{}$ = Fourier transform
$\circ$ = dot product

Subscripts

a = related to observation point a
b = related to observation point b
c = coherent
i = incident
r = real part
s = at location s

Introduction

THE statistical second moment of the electric field in random media, termed correlation, provides important information on the characteristics of the medium and the scattering particles in it.[1] From the measured correlation functions, one can determine fluid/particle properties such as particle diameter, fluid viscosity, and diffusion constant. These properties are of paramount importance in various applications such as soot formation in combustion systems.[2,3] In addition, photon correlation spectroscopy (PCS) or dynamic light scattering (DLS) has also been used to study the thermal stability of aviation fuels and the formation and growth of particles formed during the thermal degradation of the fuel.[4] However, the full potential of dynamic light-scattering techniques has not been explored because of theoretical complexities. Most of the theoretical work to date has dealt with the single-scattering limit, i.e., the Born approximation.[1,5–7]

Recently, the study of the time dependence of intensity fluctuations in the highly multiple scattering limit, termed diffusive wave spectroscopy (DWS), has been examined both theoretically and experimentally with success.[8–10] However, DWS presumes optically dense media and may not be interpreted in the intermediate scattering regime.[11] In addition, DWS theory does not consider the wave number renormalization that is caused by multiple scattering, as discussed by early researchers.[12–20]

Through multiple-scattering theory, several early researchers have established the relationship among the mean field bilinear quantities and the specific intensity of radiation.[13–18] Although the earliest paper on the subject of multiple scattering of waves dates as far back as 1945,[12] several subsequent papers have derived the radiative transport equation from the multiple-scattering theory.[13–18] Until recently,[15,20,21] the connection between the radiative transfer equation and the correlation function had not been formally recognized.

In a previous paper, Ackerson et al.[20] proposed a correlation transfer (CT) equation that was heuristically developed by modifying the radiative transfer (RT) equation. The field correlation was found to satisfy an integral equation that is formally similar to the RT equation. Exact and exponential kernel approximation methods were used to solve a preaveraged CT equation. This preaveraged form of the CT equation fits the DWS restrictions. A more rigorous derivation of the CT equation was reported by Dougherty et al.,[21] and results were presented using a three-term Legendre expansion of g^1.

In this paper, the more rigorous approach in deriving the CT equation, followed in a previous paper,[21] will be briefly outlined. This will be accomplished through a modification of the Twersky equation[16] for the mean bilinear moment of the electric field,[12,15] and with an appropriate choice of the probability density.[21]

The CT equation has the potential to cover all ranges of scattering, it can handle refractive index changes, and it also can take account of polarization effects.[22] A comparison between experimental and theoretical results will be presented for correlation in both the transmitted and backscattering directions for media of different optical thicknesses and with different indices of refraction. Results will also be presented for detection at angles other than transmitted and backscattered in the normal direction.

Development

Consider a scalar field $E(\boldsymbol{r}_a, t_a)$ that fluctuates as a random function of time t_a and at location $\boldsymbol{r}_a$, a point in the medium within a random distribution of N particles. The particles are located at $\boldsymbol{r}_1, \boldsymbol{r}_2, \ldots, \boldsymbol{r}_N$ in a specified scattering volume. It can be shown[15] that the coherent intensity is related to the average of the square of the magnitude of the electric field $E(\boldsymbol{r}_a, t_a)$, i.e.,

$$U_c(\boldsymbol{r}_a) = \langle |E(\boldsymbol{r}_a, t_a)|^2 \rangle = \int_{4\pi} I(\boldsymbol{r}_a, \hat{\boldsymbol{\Omega}}')\, d\Omega' \tag{1}$$

The angle brackets in Eq. (1) denote the ensemble average of E with respect to all particle locations $\boldsymbol{r}_1, \boldsymbol{r}_2, \ldots, \boldsymbol{r}_s, \ldots, \boldsymbol{r}_N$.

Multiple-scattering considerations lead to an equation for the time-independent spatial field correlation function, also called the mutual coherence function (MCF). In the far-field approximation, the MCF is given by[15,16]

$$\langle E(\boldsymbol{r}_a)E^*(\boldsymbol{r}_b)\rangle = \langle \boldsymbol{\phi}_i(\boldsymbol{r}_a)\rangle\langle \phi_i^*(\boldsymbol{r}_b)\rangle + \int\int_{4\pi} V(r_{as}, \hat{\boldsymbol{\Omega}}, \hat{\boldsymbol{\Omega}}')V^*(r_{bs}, \hat{\boldsymbol{\Omega}}, \hat{\boldsymbol{\Omega}}')\rho(\boldsymbol{r}_s)I(\boldsymbol{r}_s, \hat{\boldsymbol{\Omega}}')\, d\Omega'\, d\boldsymbol{r}_s \tag{2}$$

where $\rho(\boldsymbol{r}_s)$ is the probability of finding the particle s within the volume element $d\boldsymbol{r}_s$. The function V is defined by[21]

$$V(r_{as}, \hat{\boldsymbol{\Omega}}, \hat{\boldsymbol{\Omega}}') = f(\hat{\boldsymbol{\Omega}}, \hat{\boldsymbol{\Omega}}')\exp(iKr_{as})/r_{as} \tag{3}$$

where $i = \sqrt{-1}$, $r_{as}\hat{\boldsymbol{\Omega}} = (\boldsymbol{r}_a - \boldsymbol{r}_s)$, and $\hat{\boldsymbol{\Omega}}$ is a unit vector in the scattering direction $(\boldsymbol{r}_a - \boldsymbol{r}_s)$. f is related to P through the following:

$$|f(\hat{\boldsymbol{\Omega}}, \hat{\boldsymbol{\Omega}}')|^2 = (a_t/4\pi)P(\hat{\boldsymbol{\Omega}}, \hat{\boldsymbol{\Omega}}') \tag{4}$$

Note that K in Eq. (3) is an effective wave number, which is a complex number in general, and it is different from the real wave number in the scattering-free medium, $k(=2\pi n/\boldsymbol{\lambda})$. K can be approximated by[12,16]

$$K = k + 2\pi\rho f(\hat{\boldsymbol{\Omega}}, \hat{\boldsymbol{\Omega}})/k \tag{5}$$

when ρf is small, and where ρ is the average number density. This renormalization of the wave number is because of the multiple scattering in the medium as compared to single scattering.[12]

Ishimaru[15] showed how the RT equation for the specific intensity can be derived from the MCF equation [Eq. (2)] under specific conditions. When the MCF is slowly varying as a

function of the correlation distance, $\boldsymbol{r}_d = \boldsymbol{r}_a - \boldsymbol{r}_b$, it can be related to the specific intensity, $I(\boldsymbol{r}, \hat{\boldsymbol{\Omega}}')$, by[13–15]

$$\langle E(\boldsymbol{r}_a)E^*(\boldsymbol{r}_b)\rangle = \int_{4\pi} I(\boldsymbol{r}, \hat{\boldsymbol{\Omega}}')\exp(iK\hat{\boldsymbol{\Omega}}'\circ\boldsymbol{r}_d)\, \mathrm{d}\Omega' \tag{6}$$

where $\boldsymbol{r} = (\boldsymbol{r}_a + \boldsymbol{r}_b)/2$ is the c.g. coordinate.

Time-Dependent MCF

For a time-dependent field and for a particle moving within that field, among a large group of uncorrelated particles, from position and time $r_{s\blacksquare}$, $t_{s\blacksquare}$ to $r_{s'}$, $t_{s'}$ (Fig. 1), we can generalize Eq. (2) for the time-dependent MCF as[21]

$$\begin{aligned}\langle E(\boldsymbol{r}_a, t_a)E^*(\boldsymbol{r}_b, t_b)\rangle &= \langle \boldsymbol{\phi}_i(\boldsymbol{r}_a, t_a)\rangle\langle \boldsymbol{\phi}_i^*(\boldsymbol{r}_b, t_b)\rangle \\ &+ \int\int\int V(r_{as'}\hat{\boldsymbol{\Omega}}_a, \hat{\boldsymbol{\Omega}}')V^*(r_{bs\blacksquare}\hat{\boldsymbol{\Omega}}_b, \hat{\boldsymbol{\Omega}}')\Gamma(\boldsymbol{r}_s, \boldsymbol{q}, \tau) \\ &\times \exp(i\boldsymbol{q}\circ\boldsymbol{r}_{sd})w(\boldsymbol{r}_{s'}, t_{s'}|\boldsymbol{r}_{s\blacksquare}, t_{s\blacksquare})\, \mathrm{d}^3q\, \mathrm{d}\boldsymbol{r}_{s'}\, \mathrm{d}\boldsymbol{r}_{s\blacksquare}\end{aligned} \tag{7}$$

where $r_{as'}\hat{\boldsymbol{\Omega}}_a = (\boldsymbol{r}_a - \boldsymbol{r}_{s'})$, $r_{bs\blacksquare}\hat{\boldsymbol{\Omega}}_b = (\boldsymbol{r}_b - \boldsymbol{r}_{s\blacksquare})$, and w is a conditional probability of finding a particle at position $\boldsymbol{r}_{s'}$ for time $t_{s'}$, the particle being previously at position $\boldsymbol{r}_{s\blacksquare}$ for a corresponding earlier time $t_{s\blacksquare}$. $\Gamma(\boldsymbol{r}_s, \boldsymbol{q}, \tau)$ is defined by a Fourier decomposition of the time-dependent MCF[14,15]

$$\begin{aligned}\langle E(\boldsymbol{r}_{s'}, t_{s'})E^*(\boldsymbol{r}_{s\blacksquare}, t_{s\blacksquare})\rangle &\equiv \Gamma(\boldsymbol{r}_s, \boldsymbol{r}_{sd}, \tau) \\ &= \int \Gamma(\boldsymbol{r}_s, \boldsymbol{q}, \tau)\exp(i\boldsymbol{q}\circ\boldsymbol{r}_{sd})\, \mathrm{d}^3q\end{aligned} \tag{8}$$

where $\boldsymbol{q}$ represents the momentum transfer, $\tau = t_{s'} - t_{s\blacksquare}$ is the correlation delay time, $\boldsymbol{r}_s = (\boldsymbol{r}_{s'} + \boldsymbol{r}_{s\blacksquare})/2$, and $\boldsymbol{r}_{sd} = \boldsymbol{r}_{s'} - \boldsymbol{r}_{s\blacksquare}$.

If we consider the special case for which the particles slowly diffuse in a medium, the conditional probability is the Brownian motion probability function[23]

$$w(\boldsymbol{r}_{s'}, t_{s'}|\boldsymbol{r}_{s\blacksquare}, t_{s\blacksquare}) = \rho(\boldsymbol{r}_{s\blacksquare}, t_{s\blacksquare})\exp(-|\boldsymbol{r}_{s\blacksquare} - \boldsymbol{r}_{s'}|^2/4D_0\tau)/(4\pi D_0\tau)^{3/2} \tag{9}$$

Substituting Eq. (9) into Eq. (7), while assuming that $(t_a - t_b)$ is on the order of τ, we find

$$\begin{aligned}\int \Gamma(\boldsymbol{r}, \boldsymbol{q}, \tau)\exp(i\boldsymbol{q}\circ\boldsymbol{r}_d)\, \mathrm{d}^3q &= \int \Gamma_i(\boldsymbol{r}, \boldsymbol{q}, \tau)\exp(i\boldsymbol{q}\circ\boldsymbol{r}_d)\, \mathrm{d}^3q \\ &+ \int\int\int V(r_{as'}\hat{\boldsymbol{\Omega}}_a, \hat{\boldsymbol{\Omega}}')V^*(r_{as\blacksquare}\hat{\boldsymbol{\Omega}}_b, \hat{\boldsymbol{\Omega}}')\Gamma(\boldsymbol{r}_s, \boldsymbol{q}, \tau) \\ &\times \exp(i\boldsymbol{q}\circ\boldsymbol{r}_{sd})\rho(\boldsymbol{r}_{s\blacksquare}, t_{s\blacksquare})\exp(-|\boldsymbol{r}_{s\blacksquare} - \boldsymbol{r}_{s'}|^2/4D_0\tau) \\ &\times \frac{\mathrm{d}^3q\, \mathrm{d}\boldsymbol{r}_{s'}\, \mathrm{d}\boldsymbol{r}_{s\blacksquare}}{(4\pi D_0\tau)^{3/2}}\end{aligned} \tag{10}$$

where equations similar to Eq. (8) have also been substituted for the terms $\langle E(\boldsymbol{r}_a, t_a)E^*(\boldsymbol{r}_b, t_b)\rangle$ and $\langle \phi_i(\boldsymbol{r}_a, t_a)\rangle\langle \phi^* i(\boldsymbol{r}_b, t_b)\rangle$ in Eq. (7).[15]

Correlation Transfer Equation

In this section, we will employ a series of approximations similar to those used by Ishimaru[15] and shall derive the correlation transfer equation.

First, let's assume that the particles are moving with a velocity negligible as compared to the speed of light and use our assumption that $(t_a - t_b)$ is on the order of τ. Then we can set $\hat{\boldsymbol{\Omega}}_a \cong \hat{\boldsymbol{\Omega}}$ and $\hat{\boldsymbol{\Omega}}_b \cong \hat{\boldsymbol{\Omega}}$, where $\hat{\boldsymbol{\Omega}} \cong (\hat{\boldsymbol{\Omega}}_a + \hat{\boldsymbol{\Omega}}_b)/2$. For $|\boldsymbol{r} - \boldsymbol{r}_s| >> d^2/\boldsymbol{\lambda}$, this will allow us to use the following approxi-

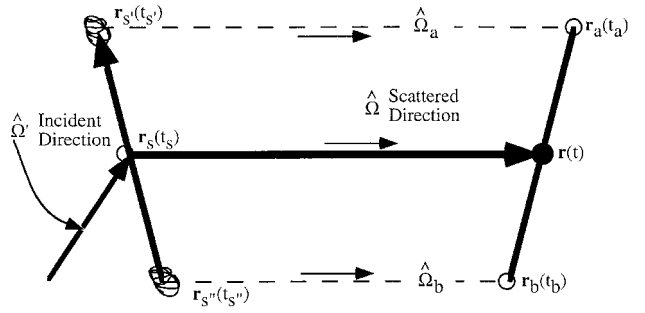

Fig. 1 Scattering geometry for a particle moving within an electric field.

mations[21] for the phase of the V functions appearing in Eqs. (3) and (10) (refer to Fig. 1)

$$2|\boldsymbol{r}_a - \boldsymbol{r}_{s'}| \cong 2|\boldsymbol{r} - \boldsymbol{r}_s| + (\boldsymbol{r}_d - \boldsymbol{r}_{sd})\circ\hat{\boldsymbol{\Omega}} \tag{11a}$$

$$2|\boldsymbol{r}_b - \boldsymbol{r}_{s\blacksquare}| \cong 2|\boldsymbol{r} - \boldsymbol{r}_s| - (\boldsymbol{r}_d - \boldsymbol{r}_{sd})\circ\hat{\boldsymbol{\Omega}} \tag{11b}$$

$$|\boldsymbol{r}_a - \boldsymbol{r}_{s'}||\boldsymbol{r}_b - \boldsymbol{r}_{s\blacksquare}| \cong |\boldsymbol{r} - \boldsymbol{r}_s|^2 \tag{11c}$$

which gives

$$\begin{aligned}V(r_{as'}\hat{\boldsymbol{\Omega}}_a, \hat{\boldsymbol{\Omega}}')V^*(r_{bs\blacksquare}\hat{\boldsymbol{\Omega}}_b, \hat{\boldsymbol{\Omega}}') &\cong (a_r/4\pi)P(\hat{\boldsymbol{\Omega}}, \hat{\boldsymbol{\Omega}}') \\ &\times \exp(-\sigma_t|\boldsymbol{r} - \boldsymbol{r}_s|)\exp(iK_r\hat{\boldsymbol{\Omega}}\circ\boldsymbol{r}_d) \\ &\times \exp(-iK_r\hat{\boldsymbol{\Omega}}\circ\boldsymbol{r}_{sd})/|\boldsymbol{r} - \boldsymbol{r}_s|^2\end{aligned} \tag{12}$$

where $K_r = (K + K^*)/2$ is the real part of K, the extinction coefficient is given by $\sigma_t = \rho a_t = i^{-1}(K - K^*)$,[15,21] Eq. (4) has been used, and ρ is assumed to be a constant.

Next, it can be shown that $\Gamma(\boldsymbol{r}, \boldsymbol{q}, \tau)$ is related to the field correlation function (G^m)[20]

$$\Gamma(\boldsymbol{r}, \boldsymbol{q}, \tau) \cong \delta(q - K_r)G^m(\boldsymbol{r}, K_r\hat{\boldsymbol{\Omega}}_q, \tau)/K_r^2 \tag{13}$$

where G^m is defined by

$$G^m(\boldsymbol{r}, K_r\hat{\boldsymbol{\Omega}}, \tau) = \langle E(\boldsymbol{r}, K_r\hat{\boldsymbol{\Omega}}, 0)E^*(\boldsymbol{r}, K_r\hat{\boldsymbol{\Omega}}, \tau)\rangle \tag{14}$$

where $\hat{\boldsymbol{\Omega}}_q(=\boldsymbol{q}/q)$ is the direction of propagation of the intensity. Substituting Eqs. (12) and (13) into Eq. (10) and introducing spherical polar coordinates in $\boldsymbol{q}$ space, i.e., $\boldsymbol{q} = q\hat{\boldsymbol{\Omega}}_q$ and $\mathrm{d}^3q = q^2\, \mathrm{d}q\, \mathrm{d}\Omega_q$, we obtain

$$\begin{aligned}\int G^m(\boldsymbol{r}, K_r\hat{\boldsymbol{\Omega}}, \tau)\exp(iK_r\hat{\boldsymbol{\Omega}}_o\boldsymbol{r}_d)\, \mathrm{d}\Omega &= \int G_i^m(\boldsymbol{r}, K_r\hat{\boldsymbol{\Omega}}, \tau)\exp(iK_r\hat{\boldsymbol{\Omega}}\circ\boldsymbol{r}_d)\, \mathrm{d}\Omega \\ &+ (\sigma_t/4\pi)\int\int\int P(\hat{\boldsymbol{\Omega}}, \hat{\boldsymbol{\Omega}}')G^m(\boldsymbol{r}_s, K_r\hat{\boldsymbol{\Omega}}', \tau) \\ &\times \exp(-|\boldsymbol{r}_{sd}|^2/4D_0\tau)\exp(-\sigma_t|\boldsymbol{r} - \boldsymbol{r}_s|)\exp(iK_r\hat{\boldsymbol{\Omega}}\circ\boldsymbol{r}_d) \\ &\times \exp[-iK_r(\hat{\boldsymbol{\Omega}} - \hat{\boldsymbol{\Omega}}')\circ\boldsymbol{r}_{sd}]\frac{\mathrm{d}\Omega'\, \mathrm{d}\boldsymbol{r}_s\, \mathrm{d}\boldsymbol{r}_{sd}}{[(4\pi D_0\tau)^{3/2}|\boldsymbol{r} - \boldsymbol{r}_s|^2]}\end{aligned} \tag{15}$$

Note that the three-dimensional integrals in the q space in Eq. (10) were reduced to solid-angle integrals in Eq. (15) because

of the delta function of Eq. (13). It should also be clear that the intensity direction $\hat{\mathbf{\Omega}}_q$ [see Eq. (13)] is equal to $\hat{\mathbf{\Omega}}$ for the scattered ray and to $\hat{\mathbf{\Omega}}'$ for the incident ray.

If, in Eq. (15), $d\boldsymbol{r}_s$ is replaced by $|\boldsymbol{r} - \boldsymbol{r}_s|^2\, dS\, d\Omega$, where dS is the elementary distance at $\boldsymbol{r}_s$ in the direction of propagation, and the integrals over the solid angle $\hat{\mathbf{\Omega}}$ are recognized to be transforms, we can equate the integrands on both sides of the equation, yielding the final equation for G^m

$$G^m(\boldsymbol{r}, K_r\hat{\mathbf{\Omega}}, \tau) = G_i^m(\boldsymbol{r}, K_r\hat{\mathbf{\Omega}}, \tau) + (\sigma_t/4\pi)\int_{r_0}^{r}\int_{4\pi} G^m(\boldsymbol{r}_s, K_r\hat{\mathbf{\Omega}}', \tau) \times g^1(K_r, \tau)P(\hat{\mathbf{\Omega}}, \hat{\mathbf{\Omega}}')\exp(-\sigma_t|\boldsymbol{r} - \boldsymbol{r}_s|)\, dS\, d\Omega' \quad (16)$$

where r_0 is a position vector on the boundary and $g^1(K_r, \tau)$ is the single-scattering field correlation function defined as[1]

$$g^1(K_r, \tau) \equiv \exp(-D_0\boldsymbol{K}_r^2\tau) = \int \exp(-|\boldsymbol{r}_{sd}|^2/4D_0\tau)\exp(-i\boldsymbol{K}_r\circ\boldsymbol{r}_{sd})\frac{d\boldsymbol{r}_{sd}}{(4\pi D_0\tau)^{3/2}} \quad (17)$$

and $\boldsymbol{K}_r = K_r(\hat{\mathbf{\Omega}} - \hat{\mathbf{\Omega}}')$. For different applications, g^1 may take different forms depending on the probability function chosen for Eq. (9).

Equation (16) is an integral equation for the field correlation function that is very similar to the radiation transfer equation for intensity, with the effective phase function being the product of P and g^1. Equation (16) reduces to the standard radiative transfer equation for the special case of zero delay time, since, for zero delay time, g^1 is unity.

Approximate Solutions of the CT Equation

In this section, we will consider only the one-dimensional case, both for finite and semi-infinite media, and develop approximate integral equations for the correlation function that will be solved using existing computer programs that were developed to solve for the intensity of radiation. We will assume azimuthal symmetry and will neglect the absorption in the medium. Under these assumptions and using optical coordinates, Eq. (16) becomes

$$G^m(z, \mu, \tau; K_r) = G_i^m(\mu, \tau; K_r) + (\omega/2)\int_0^z\int_{-1}^{1} G^m(z', \mu', \tau; K_r) \times P(\mu, \mu')g^1(K_r, \tau)\exp(-|z - z'|/\mu')\frac{d\mu'\, dz'}{\mu} \quad (18)$$

where G_i^m is the incident correlation, $z = \sigma_t\underline{z}$ is the optical coordinate, $\underline{z}$ is the physical coordinate, μ is the cosine of the polar angle (cos θ), and ω is the single-scattering albedo, which should be equal to one for pure scattering.

When the scattering particles are large compared to the wavelength, scattering is peaked in the forward direction. Thus, the phase function can be represented by a forward peak combined with an isotropic phase function[24]

$$P(\mu, \mu') = P(\cos\Theta) = 2f\delta(1 - \cos\Theta) + (1 - f) \quad (19)$$

Radiative transfer researchers have used this approximation with success in predicting laser-scattering data for the optically thick limit.[25,26] Equation (19) approximates an anisotropic phase function that has a strong forward-scattering component, such as the case for one-half-μm particles exposed to a one-half-μm wavelength laser beam. f can be computed as[24]

$$f = \left(\frac{1}{4\pi}\right)\int_{4\pi} P(\cos\Theta)\cos\Theta\, d\Omega \quad (20)$$

Substituting Eq. (19) into Eq. (18), and carrying out the preaveraging procedure[20] for g^1, which is

$$(\omega/2)\int_{-1}^{1} G^m(z, \mu', \tau; K_r)[g^1(K_r, \tau) - 1]\, d\mu' \cong \omega(2\tau/\tau_0)G^m(z, \mu, \tau; K_r) \quad (21)$$

we obtain an equation for the correlation function similar to the isotropic scattering RT equation for intensity, with the optical thickness redefined as $z = \sigma_t\underline{z}(1 - f)(1 + 2\omega\tau/\tau_0)$ and an effective albedo defined as $\omega_e = \omega/(1 + 2\omega\tau/\tau_0)$, i.e.,

$$G^m(z, \mu, \tau; K_r) = G_i^m(\mu, \tau; K_r) + (\omega_e/2) \times \int_0^z\int_{-1}^{1} G^m(z', \mu', \tau; K_r)\exp(-|z - z'|/\mu')\frac{d\mu'\, dz'}{\mu} \quad (22)$$

Note that $\tau_0 = D_0K_r^2$. Results are presented herein for Eq. (22), with a Fresnel reflective boundary condition, i.e.,[27]

$$G_i^m(\mu, \tau; K_r) = G_i(\mu) + R(\mu, n)G^m(0, \mu, \tau; K_r) \quad (23)$$

where n is a relative refractive index (i.e., the ratio of index inside the medium to index outside the medium). $G_i(\mu)$ is because of the correlation crossing the upper boundary from outside the medium, $G^m(0, \mu, \tau; K_r)$ is the contribution because of the correlation that is incident on the upper boundary from within the medium and reflected into the medium by that boundary, and Fresnel's reflection coefficient is[27]

$$R(\mu, n) = 0.5[[(s - \mu)/(s + \mu)]^2 + [(s - \mu/n^2)/(s + \mu/n^2)]^2] \quad \text{for} \quad \mu \le (1 - n^{-2})^{0.5} \quad (24a)$$

$$R(\mu, n) = 1.0 \quad \text{for} \quad \mu \ge (1 - n^{-2})^{0.5} \quad (24b)$$

where

$$s = [1 - (1 - \mu^2)n^2]^{0.5}/n \quad (24c)$$

Note that the Fresnel reflection coefficient that has been used assumes that the radiation is equally polarized in the vertical and horizontal directions. After several scattering events within the medium, an incident polarized laser beam will become depolarized. Thus, we have used a reflection coefficient that is not representative for the first few reflections of a polarized laser beam, but becomes more representative of the radiation as additional scattering events occur. Since our experimental testing was conducted for multiple-scattering situations, the reflection coefficient of Eqs. (24) should approximate those situations reasonably well.

Results

All of the experimental data that will be presented here were obtained from multiple scattering of a 514.5-μm wavelength laser beam. The sample was a 4 by 4 by 0.2 cm cell that was filled with monodisperse, micron-sized (0.107, 0.304, and 0.497 μm) latex particles in distilled water.[28] This sample was exposed to an incident expanded laser beam 4 cm in diameter to simulate one-dimensional conditions. Collection optics employed two pinholes followed by a photomultiplier tube. Absorption was assumed to be negligible for the latex particles, i.e., the single-scattering albedo was unity. Thus, the optical thickness and effective albedo reduce to $z = \sigma_s\underline{z}(1 - f)(1 + 2\tau/\tau_0)$ and $\omega_e = 1/(1 + 2\tau/\tau_0)$.

Much of the experimental results (for a backscattered correlation in multiple scattering media) demonstrate an exponential decay of correlation as a function of the square root of delay time τ.[20] Thus, in the following figures, the natural log-

arithm of $G^m(z, \mu, \tau; K_r)$ is plotted vs $(\tau/\tau_0)^{1/2}$, where τ_0 is a characteristic delay time, $\tau_0 = 1/D_0K_r^2$ ($\approx 1/D_0k^2$ for the samples used herein). For calculating the experimental τ_0, Eq. (5) shows that for small ρf (as for the experimental samples studied herein), K_r is very close to k. Thus, for all of the results presented, only k is needed for computation of τ_0.

Transmission Results

From the solution by the preaveraging technique [Eq. (22)], transmission results ($z = z_0$) in the normal direction ($\mu = 1$) are shown in Figs. 2 and 3 for 0.304-μm particle suspensions with L_0 of 5, 10, and 25, corresponding to volume fractions of 0.125, 0.25, and 0.625%, respectively. [Note that because z_0 is a function of τ/τ_0, i.e., $z_0 = \sigma_s z_0(1 - f)(1 + 2\tau/\tau_0)$, the numerical solution for correlation function at each τ/τ_0 requires the use of a different z_0. Therefore, the nominal optical thickness $\sigma_s z_0 = L_0$ is used to designate each case.] Figure 2 compares the experimental data with the approximate results of preaveraged theory. For the case of isotropic scattering ($f = 0$) and unit index of refraction ($n = 1$), the data and theory are in poor agreement, with the theory predicting a much faster decay rate than that measured. This is expected because, in addition to preaveraging, the effects of anisotropy and refractive index were neglected.

When the forward-scattering approximation is employed ($f = 0.727$, which was computed from Mie theory[28] for this particle/laser wavelength combination), as shown in Fig. 2, the deviation of the predictions from the experimental data is much less than that from isotropic theory. In fact, the theoretical results have changed so dramatically that they show a slower decay rate than the experimental results. However, Fig. 3 shows that keeping the isotropic assumption ($f = 0$) and using an index of refraction different than one ($n = 1.331$) at the incident light boundary leads to a slightly poorer agreement, i.e., an increased theoretical decay rate, with the experimental data than for isotropic scattering and unit refractive index (as from Fig. 2). (We have found that modeling the two air–glass–sample interfaces as a single effective interface, between air and the sample, has yielded satisfactory predictions.) Thus, it appears that for constant L_0, the forward-scattering approximation and the refractive index modeling have opposite effects on the theoretical decay rate of G^m, which suggests that

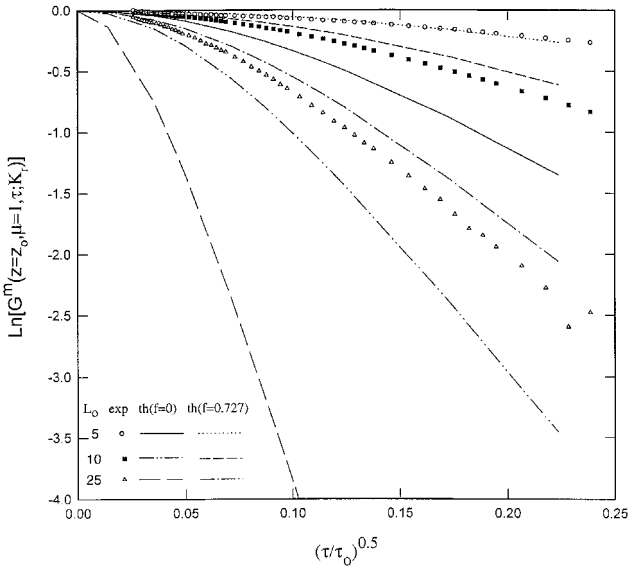

Fig. 2 Transmission ($z = z_0$, $\mu = 1.0$): comparison of experimental data with isotropic preaveraged theory ($f = 0$, $n = 1.0$) and anisotropic preaveraged theory ($f = 0.727$, $n = 1.0$) for three optical thicknesses, using 0.304-μm spheres in suspension and a laser wavelength of 514.5 nm.

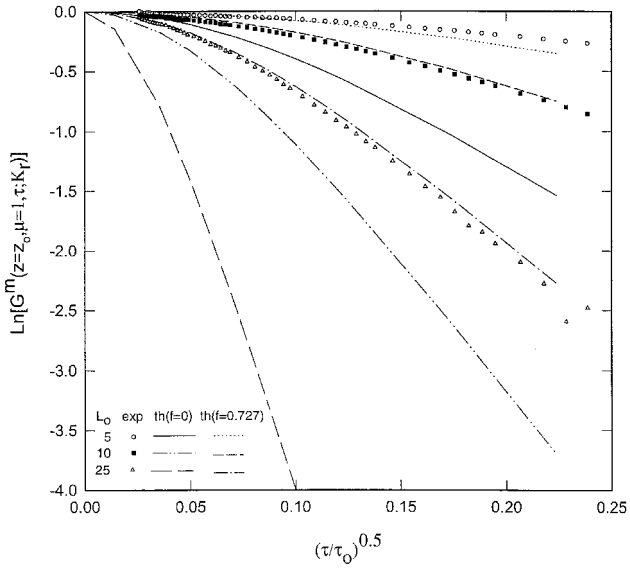

Fig. 3 Transmission ($z = z_0$, $\mu = 1.0$): comparison of experimental data with isotropic preaveraged theory ($f = 0$, $n = 1.331$) and anisotropic preaveraged theory ($f = 0.727$, $n = 1.331$) for three optical thicknesses, using 0.304-μm spheres in suspension and a laser wavelength of 514.5 nm.

a combination of the two might superpose to better match the data.

Figure 3 also includes a comparison between experiment and theory for the transmission results of the correlation function when an index of refraction of 1.331 at the boundary is assumed in the theory, and the forward-scattering approximation for the phase function [Eq. (19)] is employed with $f = 0.727$. The theory is in much better agreement with the data as compared to predictions where one or the other of these effects is neglected (Figs. 2 and 3). Although these results are only for 0.304-μm particle suspensions and use a simplified theory, they are very promising, and seem to indicate that correlation may be applicable to a great range of scattering, from single scattering to highly multiple scattering. A later section will show results for other particle sizes.

Note that the fit of the data to the theory is better for large optical thickness than for small thickness. This general trend carries through the majority of our results and suggests that another parameter may be affecting the results at small optical thicknesses. One distinct possibility is polarization, which is not included in this analysis; but a preliminary discussion of this topic can be found in Ref. 22.

Backscattering Results

In Figs. 4 and 5, theoretical results and experimental data for normal backscattering [$z = 0$ and $\mu = -1$ in Eq. (22)] are presented for finite media composed of 0.304-μm particle suspensions having L_0 of 5, 10, and 25.

For one set of theoretical curves in Fig. 4, the scattering is assumed to be isotropic ($f = 0$), and the index of refraction is set equal to unity in the preaveraged theory. As expected from the transmission results, this leads to poor agreement between theory and experiment. However, it is worth noting that for the case of an optical thickness equal to 25 the theory presents the least disagreement with the data. This could be explained by the very large number of multiple-scattering events that occur in this optically thick medium where, even for strongly anisotropic scattering, all propagation directions become equally likely, and hence, the effective scattering approaches the isotropic limit.

When the forward-scattering approximation [Eq. (19), $f = 0.727$] is included in the theory, as shown by the second set of theoretical curves in Fig. 4, the agreement with experiment

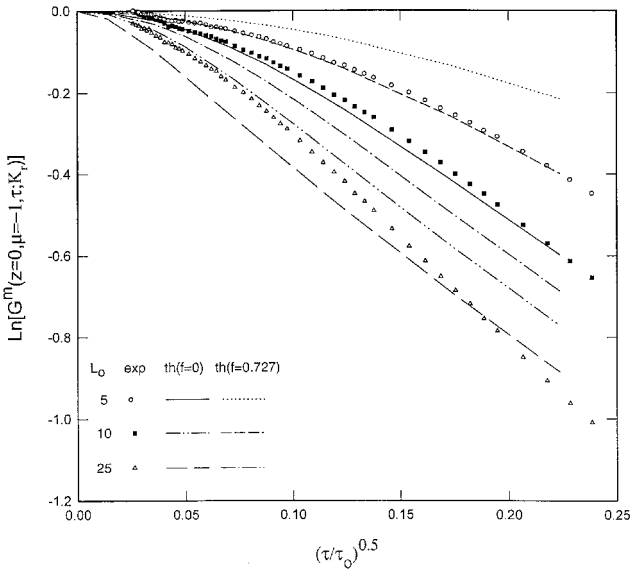

Fig. 4 Backscattering ($z = 0$, $\mu = -1.0$): comparison of experimental data with isotropic preaveraged theory ($f = 0$, $n = 1.0$) and anisotropic preaveraged theory ($f = 0.727$, $n = 1.0$) for three optical thicknesses, using 0.304-μm spheres in suspension and a laser wavelength of 514.5 nm.

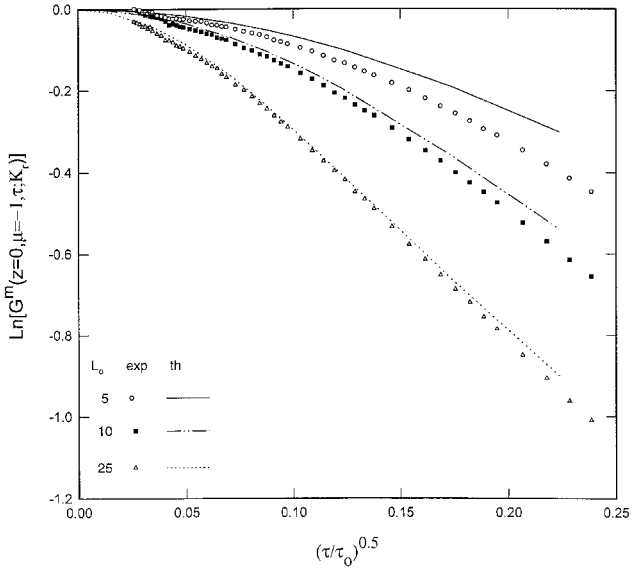

Fig. 5 Backscattering ($z = 0$, $\mu = -1.0$): comparison of experimental data with anisotropic preaveraged theory ($f = 0.727$, $n = 1.331$) for three optical thicknesses, using 0.304-μm spheres in suspension and a laser wavelength of 514.5 nm.

is improved as compared to the isotropic theory. When both the effects of refractive index ($n = 1.331$) at the boundary and anisotropic scattering ($f = 0.727$) are included in the theory, the agreement with the experiment is much better as shown in Fig. 5. As with transmission, the poorest agreement is at small optical thickness. Note that these results and those for transmission are shown for relatively short nondimensional delay time ratios [$(\tau/\tau_0)^{1/2} < 0.25$ or $\tau/\tau_0 < 0.0625$], and this is in keeping with the preaveraging assumption [Eq. (21)] of the correlation equation.[20]

Additional Particle Sizes

Figures 6–9 compare transmission and backscattering theory to data for 0.497- and 0.107-μm particles, considering nominal optical thicknesses of 3, 5, and 7 (corresponding to volume fractions of 0.54, 0.90, and 1.26%, respectively). In these figures, the anisotropic factor and refractive index are also included in the theory. Figures 6 and 7 give the transmission and backscattering results for the 0.497-μm particle suspensions ($L_0 = 10$, 20, and 30 correspond to volume fractions of 0.14, 0.29, and 0.43%, respectively), showing matches between theory and data that are not quite as good as those for the 0.304-μm particles. Nevertheless, the theory does a reasonable job of predicting the data, especially for large optical thickness, and demonstrates that the simple preaveraging theory works quite well if refractive index and anisotropy are included. The data and theory for 0.107-μm-diam particles are presented in Figs. 8 and 9 for transmission and backscattering, respectively. The quality of match with data for transmission is similar to that for the 0.304- and 0.497-μm particles. However, the 0.107-μm particle theory does not predict data well for backscattering. This may be partially because of the much smaller optical thicknesses that were investigated for 0.107-μm particles than for the 0.304- and 0.497-μm particles. The

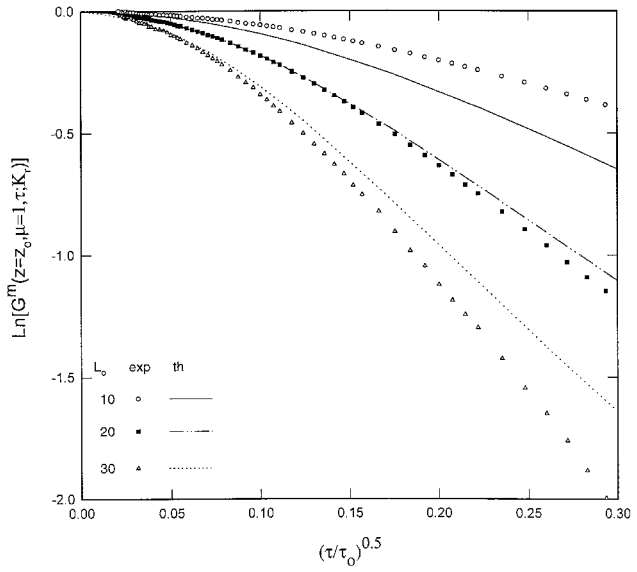

Fig. 6 Transmission ($z = z_o$, $\mu = 1.0$): comparison of experimental data with anisotropic preaveraged theory ($f = 0.858$, $n = 1.331$) for three optical thicknesses, using 0.497-μm spheres in suspension and a laser wavelength of 514.5 nm.

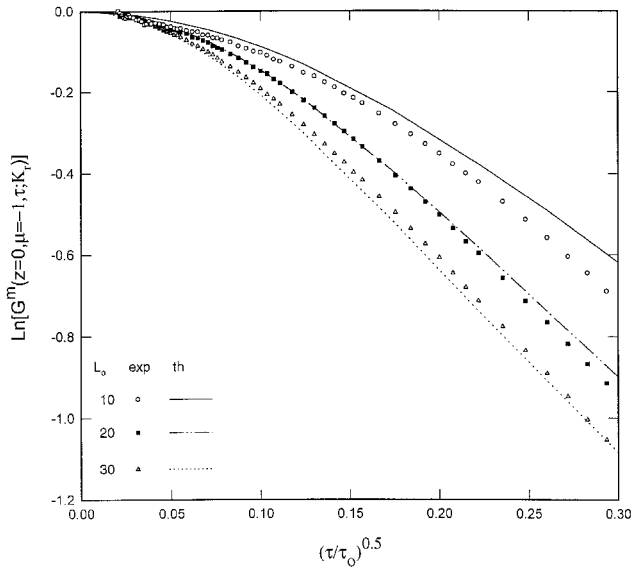

Fig. 7 Backscattering ($z = 0$, $\mu = -1.0$): comparison of experimental data with anisotropic preaveraged theory ($f = 0.858$, $n = 1.331$) for three optical thicknesses, using 0.497-μm spheres in suspension and a laser wavelength of 514.5 nm.

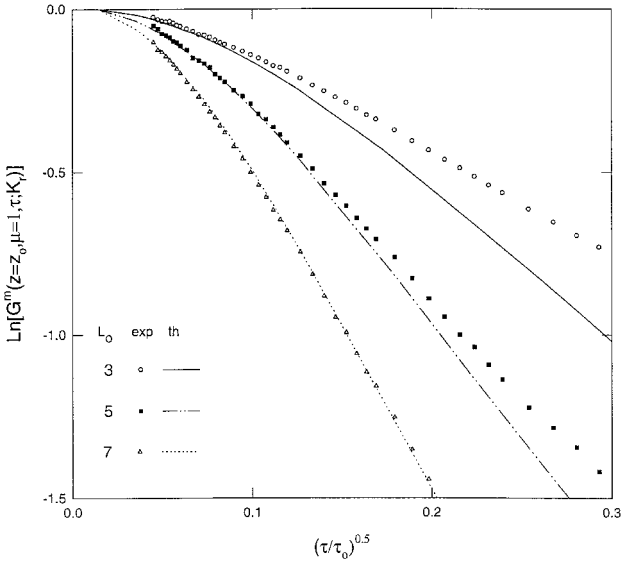

Fig. 8 Transmission ($z = z_o$, $\mu = 1.0$): comparison of experimental data with anisotropic preaveraged theory ($f = 0.132$, $n = 1.331$) for three optical thicknesses, using 0.107-μm spheres in suspension and a laser wavelength of 514.5 nm.

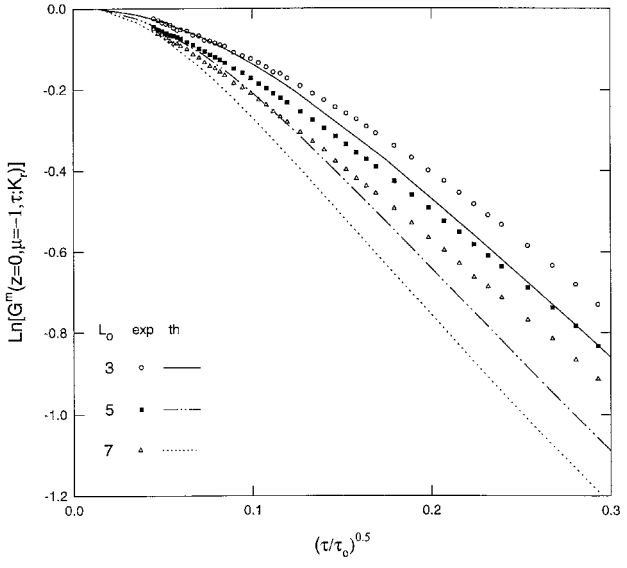

Fig. 9 Backscattering ($z = 0$, $\mu = -1.0$): comparison of experimental data with anisotropic preaveraged theory ($f = 0.132$, $n = 1.331$) for three optical thicknesses, using 0.107 μm spheres in suspension and a laser wavelength of 514.5 nm.

smaller optical thicknesses may have allowed single-scattering polarization effects (not included in this theory) to play a greater role in backscattering than in transmission.

Nonnormal Detection

The effects of nonnormal detection measurements on the field correlation function are presented in Fig. 10 for transmission ($\mu > 0$) from samples with optical thicknesses of 5 and 10 (0.304-μm particle suspensions). For an optical thickness of 5 it can be seen that, as detection angle differs greatly from direct transmission, there is a slight but decided increase in decay rate. For an optical thickness of 10 this effect is much smaller, with the theory having the same trend as for an optical thickness of 5; whereas the data do not show a clear trend. Since the spread in data (and theory) for an optical thickness of 10 is so small, this probably indicates the limits of accuracy with which the data can be taken.

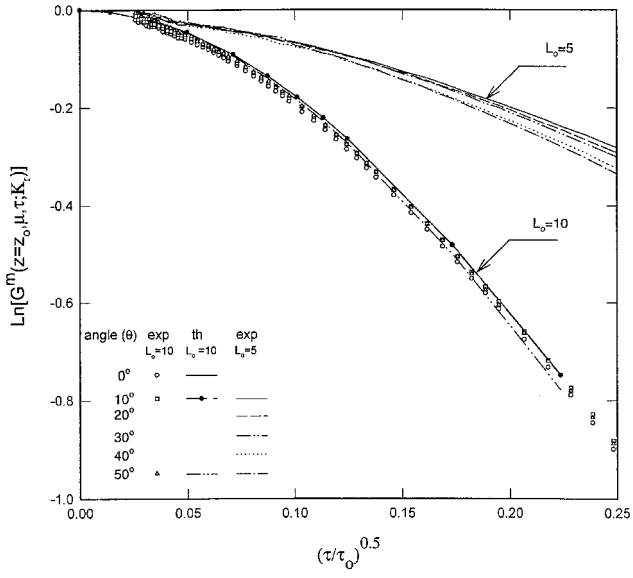

Fig. 10 Transmission ($z = z_o$, $\mu = 1.0$): effect of detection angle on experimental data for optical thickness of 5 and 10; and comparison of this experimental data with anisotropic preaveraged theory ($f = 0.727$, $n = 1.331$) for an optical thickness of 10, using 0.304-μm spheres in suspension and a laser wavelength of 514.5 nm.

The backscattered experimental measurements are not presented because there are no decipherable differences among the direct backscattered theory curves as a function of detection angle and the data also show very little differences (for an optical thickness of 10). Therefore, just as with transmission, only small optical thicknesses will exhibit decay rate changes with detection angle; and even these effects appear to be rather minor.

Comparison with Other Theories

We have compared CT theory with DWS theory in Refs. 20 and 21. In those publications, infinite optical thickness, i.e., a diffusion limit, CT theory was shown to compare well with DWS, as expected. Since DWS was specifically derived for the diffusion limit we do not expect DWS to compare well to CT or to data for the small to intermediate optical thicknesses studied herein. In addition to the preaveraging technique that we have investigated, other approximate radiative transfer solution techniques have been applied to dynamic light scattering in multiple-scattering media. One such technique is the two-stream approximation.[29] In one dimension, this method assumes two intensities, one in the positive direction and one in the negative direction, similar to the two-flux approximation. However, as applied to correlation problems, the equations must be solved for intensity, not for flux.

Shown in Figs. 11 and 12 are the transmission and backscattering results for CT and the two-stream theory[29] compared to our data. In the two-stream equations of Ref. 29, the average reflecting probability of diffusing photons was taken as 0.4522 (suggested by the author to account for the two interfaces, sample–glass and glass–air), the deposition depth was two-thirds, the anisotropic factor (f) was 0.727, and the ballistic reflection probability was taken to be zero. As can be seen by examining Fig. 11, CT is a slightly better predictor for transmission data. Although Ref. 29 does not present a final equation for backscattered correlation function, it is possible to obtain that equation by following a procedure similar to that used in obtaining the two-stream transmission function. Integrating the appropriate Ref. 29 backscattering equation yields the results of Fig. 12, which compares two-stream theory to CT theory and our data. As can be seen, while CT theory predicts

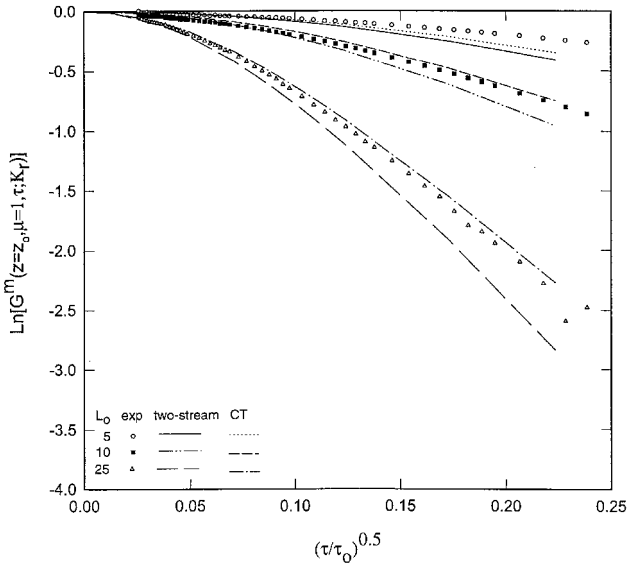

Fig. 11 Backscattering ($z = 0$, $\mu = -1.0$): comparison of preaveraged CT theory ($f = 0.727$, $n = 1.331$), two-stream theory (diffusive reflectivity = 0.4522, $f = 0.727$, deposition depth = 2/3, and ballistic reflectivity = 0.0), and experimental data for optical thicknesses of 5, 10, and 25; using 0.304-μm spheres in suspension and a laser wavelength of 514.5 nm.

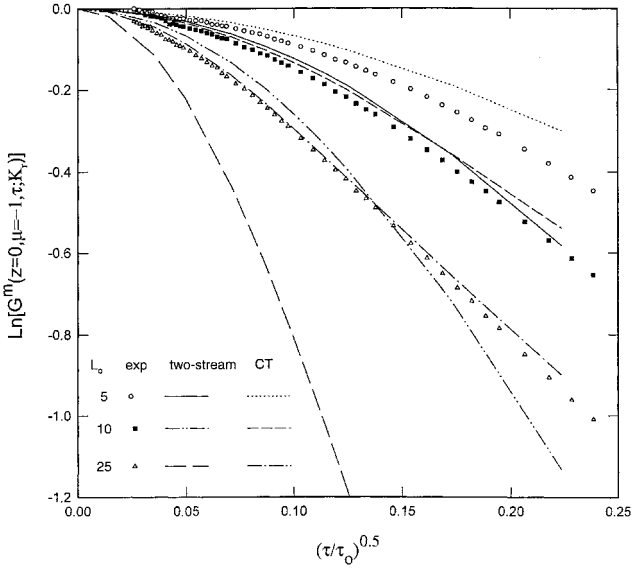

Fig. 12 Transmission ($z = z_o$, $\mu = 1.0$): comparison of preaveraged CT theory ($f = 0.727$, $n = 1.331$), two-stream theory (diffusive reflectivity = 0.4522, $f = 0.727$, deposition depth = 2/3, and ballistic reflectivity = 0.0), and experimental data for optical thicknesses of 5, 10, and 25; using 0.304-μm spheres in suspension and a laser wavelength of 514.5 nm.

the data reasonably well, the two-stream theory appears inaccurate.

Conclusions

The correlation of the temporal fluctuations of an electric field in multiple-scattering media has been shown to be governed by an integral equation similar to the radiative transport equation. To examine the effects of optical thickness, refractive index, anisotropy, and detection angle, an approximate technique (termed preaveraging, of the single-scattering correlation function) was applied to obtain simplified solutions for the electric field correlation function in isotropic and anisotropic one-dimensional media. Preliminary results indicate that the resulting theory can predict data quite well for 0.107-, 0.304-, and 0.497-μm-diam polystyrene latex scatterers suspended in liquids.

Optical thicknesses from 5 to 30 have been investigated, and agreement of data and theory is good, with the agreement generally improving as optical thickness increases. Accounting for the index of refraction changes and employing a forward-scattering approximation (isotropic scattering plus a forward spike) as a first approximation for the anisotropic scattering character of small particles in suspensions, is necessary for the preaveraged results to match data for short delay times. Employing this very simple approximation for the phase function has led to quite reasonable predictions of the experimental data. Thus, for some applications, this approximation may reduce the complication of using a more complex approximation of the phase function.

Since CT has been shown to compare well with both the data and DWS theory for diffusive cases,[20,21] our interest currently is in those ranges between optically thin and diffusive. From the results presented herein, CT has also demonstrated better predictive capability for the intermediate optical thickness data than a two-stream[29] theory. However, CT does not fit the data as well as expected for low optical thicknesses, and we believe that this may be because of polarization playing a critical role in these cases. A first step has been taken in adding simplified polarization to CT,[22] and future work will see the addition of full-fledged polarization.

Acknowledgments

The authors are grateful to the National Science Foundation for Grant CTS 9117288 and to the Oklahoma Center for the Advancement of Science and Technology for Grants AR09-20, RE9-003, and AR5-055.

References

[1]Berne, B. J., and Pecora, R., *Dynamic Light Scattering*, Wiley, New York, 1976.

[2]Charalampopoulos, T. T., and Chang, H., "In Situ Optical Properties of Soot Particles in the Wavelength Range from 340 nm to 600 nm," *Combustion Science and Technology*, Vol. 59, Nos. 4–6, 1988, pp. 401–421.

[3]Flower, W. L., "Optical Measurements of Soot Formation In Premixed Flames," *Combustion Science and Technology*, Vol. 33, Nos. 1–4, 1983, pp. 17–33.

[4]O'Hern, T. J., Trott, W. M., Martin, S. J., and Klavetter, E. P., "Advanced Diagnostics in Situ Measurements of Particle Formation and Deposition in Thermally Stressed Jet Fuels," AIAA Paper 93-0363, Jan. 1993.

[5]Pusey, P. N., and Tough, R. J. A., *Dynamic Light Scattering and Velocimetry: Applications of Photon Correlation Spectroscopy*, edited by R. Pecora, Plenum, New York, 1985.

[6]Weiner, B. B., "Particle Sizing Using Photon Correlation Spectroscopy," *Modern Methods of Particle Size Analysis*, edited by H. G. Barth, New York, 1984.

[7]Chu, B., *Laser Light Scattering*, Academic, New York, 1974.

[8]Weitz, D. A., and Pine, D. J., "Diffusing-Wave Spectroscopy," *Dynamic Light Scattering: the Method and Some Applications*, edited by W. Brown, Oxford Univ. Press, Oxford, England, UK, 1993.

[9]Pine, D. J., Weitz, D. A., Maret, G., Wolf, P. E., Herbolzheimer, E., and Chaikin, P. M., "Dynamical Correlations of Multiply Scattered Light," *Scattering and Localization of Classical Waves in Random Media*, edited by P. Sheng, World Scientific Press, London, 1990.

[10]Durian, D. J., "Penetration Depth for Diffusing-Wave Spectroscopy," *Applied Optics*, Vol. 34, No. 30, 1995, pp. 7100–7105.

[11]Yoo, K. M., Liu, F., and Alfano, R. R., "When Does the Diffusion Approximation Fail to Describe Photon Transport in Random Media?" *Physical Review Letters*, Vol. 64, No. 22, 1990, pp. 2647–2650.

[12]Foldy, L. L., "The Multiple Scattering of Waves," *Physical Review*, Vol. 67, Nos. 3/4, 1945, pp. 107–119.

[13]Barabanenkov, Y. N., "On the Spectral Theory of Radiation Transport Equations," *Soviet Physics—JETP*, Vol. 29, No. 4, 1969, pp. 679–684.

[14]Barabanenkov, Y. N., Kravtsov, Y. A., Rytov, S. M., and Tamarskii, V. I., "Status of the Theory of Propagation of Waves in a Randomly Inhomogeneous Medium," *Soviet Physics Uspekhi*, Vol. 13, No. 5, 1971, pp. 551–680.

[15]Ishimaru, A., *Wave Propagation and Scattering in Random Media*, Vols. 1 and 2, Academic, New York, 1978.

[16]Twersky, V., "On Propagation in Random Media of Discrete Scatterers," *Proceedings of the American Mathematical Society Symposium on Stochastic Processes in Mathematical Physics and Engineering*, Vol. 16, American Mathematical Society, Providence, RI, 1964, pp. 84–116.

[17]Furustu, K., "Multiple Scattering of Waves in a Medium of Randomly Distributed Particles and Derivation of the Transport Equation," *Radio Science*, Vol. 10, No. 1, 1975, pp. 29–44.

[18]Wolf, E., "New Theory of Radiative Energy Transfer in Free Electromagnetic Fields," *Physical Review D*, Vol. 13, No. 4, 1976, pp. 869–886.

[19]Lax, M., "Multiple Scattering of Waves," *Reviews of Modern Physics*, Vol. 23, No. 4, 1951, pp. 287–310.

[20]Ackerson, B. J., Dougherty, R. L., Reguigui, N. M., and Nobbmann, U., "Correlation Transfer: Application of Radiative Transfer Solution Methods to Photon Correlation Problems," *Journal of Thermophysics and Heat Transfer*, Vol. 6, No. 4, 1992, pp. 577–588.

[21]Dougherty, R. L., Ackerson, B. J., Reguigui, N. M., Dorri-Nowkoorani, F., and Nobbmann, U., "Correlation Transfer — Development and Application," *Journal of Quantitative Spectroscopy and Radiative Transfer*, Vol. 52, No. 6, 1994, pp. 713–727.

[22]Reguigui, N. M., Ackerson, B. J., Dorri-Nowkoorani, F., Nobbmann, U., and Dougherty, R. L., "Correlation Transfer: A Preliminary Investigation of the Polarization Effects," AIAA Paper 95-2020, June 1995.

[23]Kac, M., *Probability and Related Topics in Physical Sciences*, Wiley-Interscience, New York, 1957.

[24]Van de Hulst, H. C., *Multiple Light Scattering, Tables, Formulas, and Applications*, Vol. 2, Academic, New York, 1980.

[25]Look, D. C., Jr., Nelson, H. F., and Crosbie, A. L., "Anisotropic Two-Dimensional Scattering: Comparison of Experiment with Theory," *Journal of Heat Transfer*, Vol. 103, No. 1, 1981, pp. 127–134.

[26]Nelson, H. F., Look, D. C., Jr., and Crosbie, A. L., "Two-Dimensional Back-Scattering from Optically Thick Media," *Journal of Heat Transfer*, Vol. 108, No. 3, 1986, pp. 619–625.

[27]Reguigui, N. M., and Dougherty, R. L., "Two-Dimensional Radiative Transfer in a Cylindrical Layered Medium with Reflecting Boundaries," *Journal of Thermophysics and Heat Transfer*, Vol. 6, No. 2, 1992, pp. 232–241.

[28]Dorri-Nowkoorani, F., Nobbmann, U., Ackerson, B. J., Dougherty, R. L., and Reguigui, N. M., "Correlation Measurements of a Multiply Scattered Laser Beam by Fluid/Particle Suspensions, AIAA Paper 93-2745, July 1993.

[29]Durian, D. J., "Two-Stream Theory of Diffusing Light Spectroscopies," *Physica A, Statistical and Theoretical Physics*, Vol. 229, No. 2, 1996, pp. 218–235.